Investigating the Extent and Possible causes of Western Redcedar Dieback throughout its Range

Evaluation Monitoring Project Report (WC-EM-20-02)

Christine Buhl (Oregon Department of Forestry), Melissa Fischer (Washington Department of Natural Resources), and Betsy Goodrich (USFS Forest Health Protection)

March 2022

Project Summary: "We propose developing a user-friendly survey tool and utilizing a multi-agency cooperative network to map the distribution of WRC dieback and lay groundwork for more focused sampling of mortality-causing agents."

Product list:

1. Geographic extent of WRC dieback (OR, WA)
   - ✓ S123 + iNaturalist map with ground-verified WRC dieback locations
2. Network of locations with known WRC dieback for future sampling
   - ✓ S123 locations (n =369) and plots (n = 147), as well as mapped areas and a cultivated list of sites for longer-term monitoring
3. List of probable environmental and site characteristics associated with WRC dieback
   - ✓ Exploratory categorical decision tree analyses selected several environmental variables as predictors of sites with dieback
   - ✓ Statistical analyses found site factors associated with region-specific dieback
4. Permanently tagged tree/site used to monitor/photograph dieback over time
   - ✓ S123 plots
5. User-friendly, web-based survey tool (Survey123) with standardized protocols to record dieback
   - ✓ S123 form and written protocol (https://arcg.is/b9Xrr)
6. Standardized methodology and protocol instructions
   - ✓ Written protocol (https://arcg.is/b9Xrr) and video (https://youtu.be/3JgfxTJ7Jag)
7. Outreach products documenting extent of dieback and site/environmental results
   - ✓ Storymap: https://arcg.is/ezSaf
   - ✓ Dashboard: https://arcg.is/0em1Xv0
8. Presentations at 2021 National FHM meeting and 2021 WIFDWC climate change virtual meeting
   - ✓ SAF 2021 poster
   - ✓ Presented progress report at 2021 WIFDWC Climate Change Meeting (larger meeting cancelled)
   - ✓ 33 additional outreach and professional presentations
9. ADS and FIA 'heads-up': Specific coordinates provided to ADS and FIA for recording WRC dieback
   - ✓ Heads-up layer of WRC dieback points and polygons provided to Danny DePinte for conversion to a TPK layer (February 2022)

10. Bonus products and collaborations:
    - ✓ Created data collection template adapted by WSU Extension for an iNaturalist citizen science group to enhance community engagement and broaden data collection
    - ✓ Assisted with creation of a WRC summit attended by researchers and natural resource specialists in U.S. and Canada
    - ✓ Sponsored Washington State University researchers for USFS Emerging Pests funding for dendrochronology analyses, and provided dieback sampling sites and field time for researchers
    - ✓ Contributing to WRC dieback synthesis publication led by Washington State University in spring 2022

Issues or follow-up needed to quantify/complete the full extent of WRC dieback:

- No collaborator plots/input from BC or Idaho
- Inadequate sampling of WA Olympic Peninsula

Investigating the extent and possible causes of western redcedar dieback throughout its range:
Additional information to support final Evaluation Monitoring project report (WC-EM-20-02)

Scope of the dieback issue

Forest health specialists, forest landowners, and land managers have been observing western redcedar (WRC) dieback from OR through western Canada in recent years. Groups of WRC with evidence of dieback have even been observed across most of the range, often in areas which they normally thrive such as along streams and in shaded areas. The cause(s) for this sometimes sudden and expanding dieback is unknown and the focus of our project. Unfortunately, dieback symptoms vary widely and are not easily visible during aerial detection survey, where this type of damage is typically recorded, therefore the extent is unknown, but it appears to be occurring range-wide.

Some symptoms include thinning crowns, branch dieback, branch flagging, recent topkill, chlorosis (yellow foliage), heavy cone crops and mortality (Figure 1).

Fig. 1: Thinning **Flagging** **Topkill** **Yellowing**

Biological stressors

Western redcedar is fairly insect and disease resistant. Insects that infest WRC are typically secondary, meaning that they are not aggressive tree-killing species, but are opportunistic pests and can only attack dead and dying redcedar. When healthy, redcedar can resist endemic levels of bark beetles (*Phloeosinus* spp.) and woodboring beetles (*Semanotus amethystinus, Trachykele blondeli, Chrysobothris nixa,* etc.). While heartwood decay is commonly present in WRC, the species contains terpenoid chemical defense compounds (thujone and thujaplicin) and also the use sap as a mechanical barrier that make it resistant to many common decay fungi. Western redcedar is susceptible to various root and butt rot pathogens (*Postia sericeomollis, Coniferiporia weirii, Armillaria ostoyae*) and often has extensive heart rot, but primary diseases have not been visibly present at most sites where dieback has been observed. Novel

insects or diseases have not been observed and are not considered the main causal agents of this dieback epidemic.

Abiotic stressors

Given the apparent range-wide dieback and lack of consistent biotic factors, we hypothesize that the dieback is associated with abiotic causes. The PNW has been seeing increased droughty periods, especially during the summer months (Figure 2), and an increase in temperature. We hypothesize that WRC are experiencing dieback in areas where warmer, drier conditions are occurring and/or in areas where more frequent droughts affect the species ability to access water during the growing season. We also hypothesize that site factors that predispose trees to warmer, drier environments (i.e. south-facing slopes, lower elevation, etc.) may be factors contributing to dieback.

OREGON

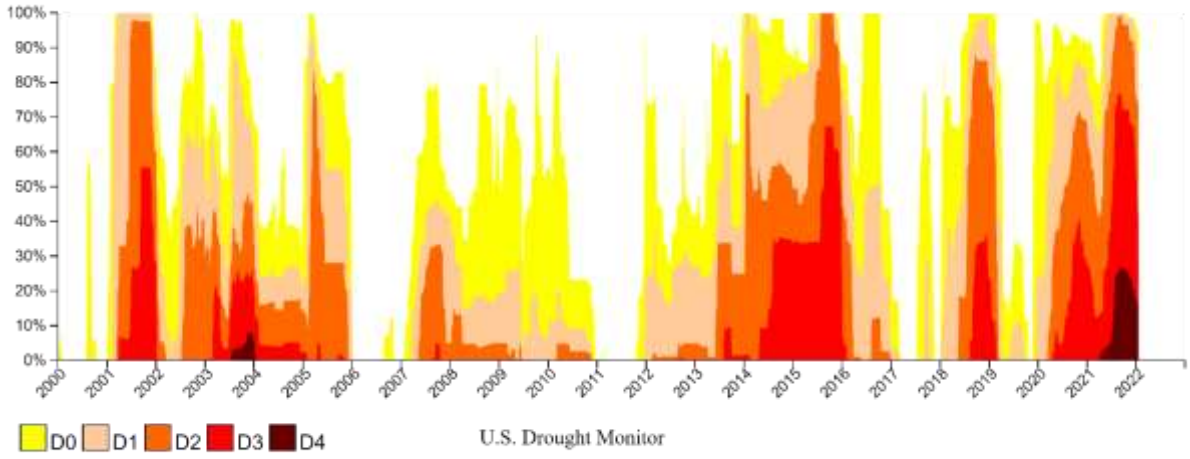

WASHINGTON

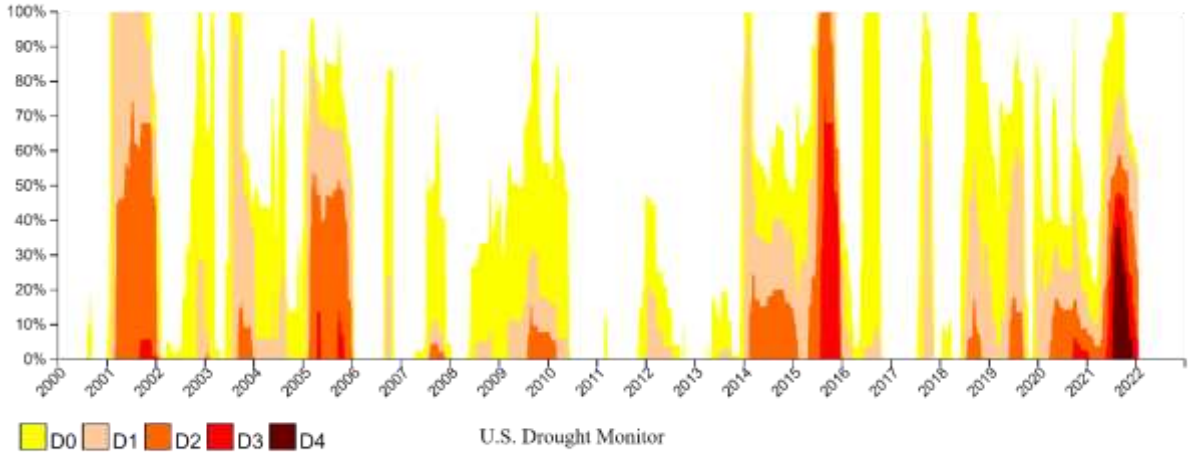

Figure 2. Oregon and Washington percent areas in U.S. Drought Monitor categories (D0=Abnormally Dry, D1=Moderate Drought, D2=Severe Drought, D3=Extreme Drought, D4=Exceptional Drought) from 2000 through 2021. https://droughtmonitor.unl.edu/

Western redcedar appears to be sensitive to a changing climate. A range of time periods and General Circulation Models (Table 1 from Crookston et al. 2009) were chosen for display below (Figure 3: a through d): a. current range (circa 2010) of *Thuja plicata*, b. predicted range in 2030 under scenario B1, c. predicted range in 2030 under scenario A2, and d. predicted range in 2090 under scenario A2. Note that even the 'best case scenario' B1 illustrates some loss of preferential habitat in western WA and OR, while models seem to agree that interior preferential habitat may expand east and north.

Table 1
General circulation models (GCM) and special report on emission scenarios (SRES) used herein.

GCM name	Center name
CGCM3	Canadian Center of Climate Modeling and Analysis
HADMC3	Met Office Hadley Centre (UK)
GFDLCM21	Geophysical Fluid Dynamics Laboratory (Princeton University, NOAA Research)
SRES scenario	**Description**
A2	High emissions, regionally diverse world, rapid growth
A1B	Intermediate emissions, homogeneous world, rapid growth
B2	Lower emissions, local environmental sustainability
B1	Lowest emissions, global environmental sustainability

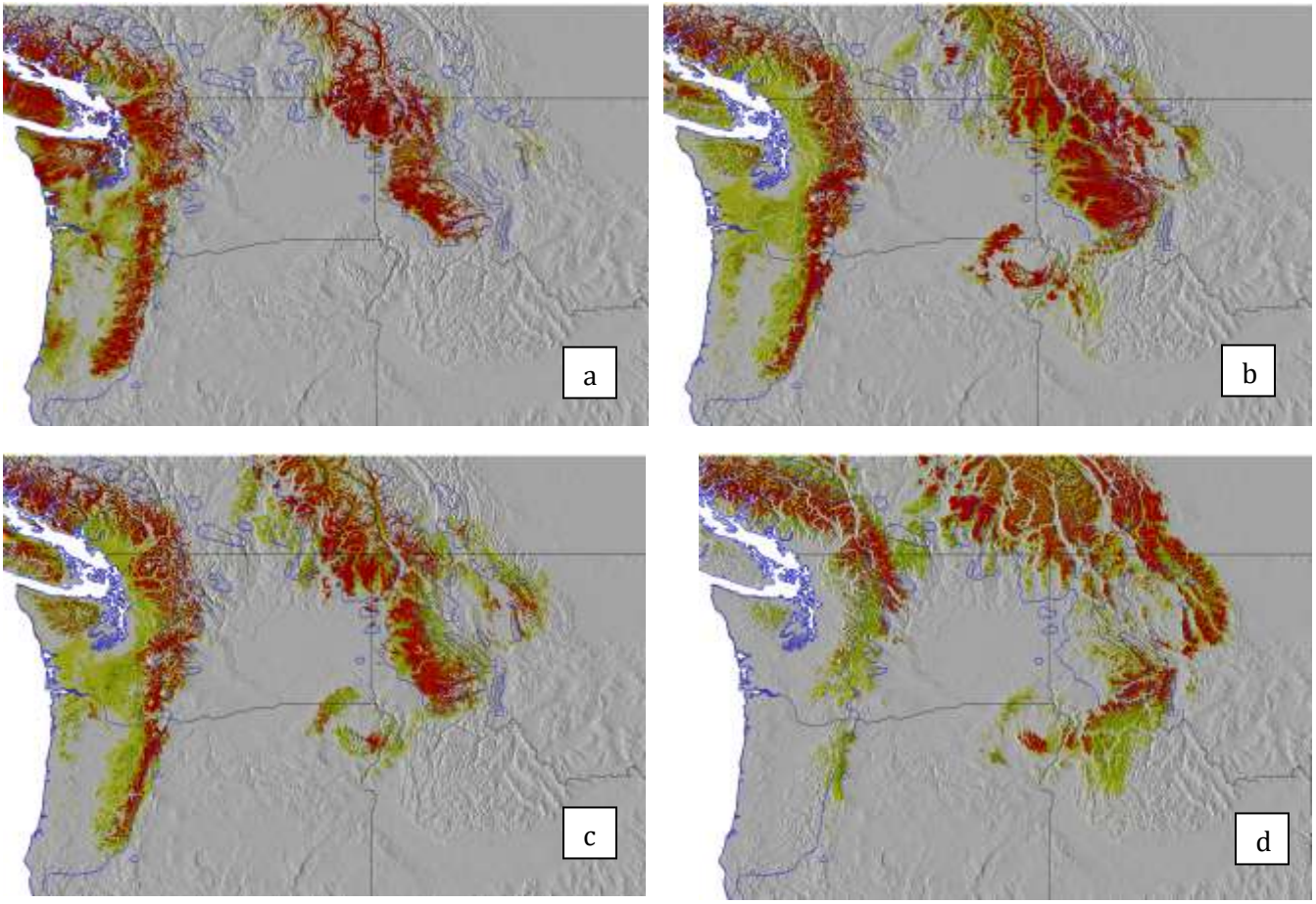

Figure 3. WRC current and predicted range (habitat favorability increases yellow < green < red [most preferred]): a. current range (circa 2010) of *Thuja plicata*, b. predicted range in 2030 under scenario B1, c. predicted range in 2030 under scenario A2, and d. predicted range in 2090 under scenario A2. *Plant Species and Climate Profile Predictions using Canadian Center of Climate Modeling and Analysis model scenarios from Crookston et al. 2009. (Maps of all tested models: https://charcoal2.cnre.vt.edu/climate/species/speciesDist/Western-redcedar/)*

Evaluation monitoring project phases, methods, and questions

Phased data collection

Determine the distribution and extent of WRC dieback across PNW using Survey123

- Locations – build a network of sites
- Record symptoms – are they common across sites?
- How quickly do trees die following initial symptoms?
- What site factors are associated with dieback (topography, slope position, etc.)
- Are there any common biotic damage agents across the range?

Determine potential causal agents

- Determine if WRC dieback has associations with geography, soils, environment, climate/weather, topography, site info, etc.
- Large scale (course resolution) soils, climate, topography, veg models included as possible covariates

Site network available for more in-depth investigations of site-specific causal agents (future research)

- More site specific investigations of dieback
- Change over time (PIs have committed to continue monitoring a subset of plots)
- Tree dissections (e.g. rings collected at various stem heights, close inspections of dying/dead tops), in-depth root investigations (e.g. depth and area of roots)
- Detailed soils information
- Physiology in various canopy positions
- Use dendrochronology (tree cores) to determine if reduced growth or dieback severity associated with specific drought years/months

Defining the distribution and extent of WRC dieback in the Pacific Northwest

A total of 369 dieback sites in WA and OR were identified by using Survey123 and of these, plots with tree and site data were established at 147 sites (Figure 5). Our goal was to establish a minimum of 10-15 plots across the range of WRC throughout respective service areas, and we exceeded that number. Data collected at each plot included both tree data (e.g. DBH, estimated age based on pictorial evidence, crown transparency and dieback levels, crown class) and stand data (e.g. total basal area and basal area of symptomatic WRC, aspect, slope position). Growth rates were approximated by collecting increment cores and counting the number of annual growth rings within several predetermined diameter growth categories or DGC (e.g., 0.25, 0.5, 1.0, 2.0 inch lengths of most recent diameter growth) (see Figure 4). One WRC at each plot was often permanently tagged for future monitoring and photographic documentation of the progression of dieback.

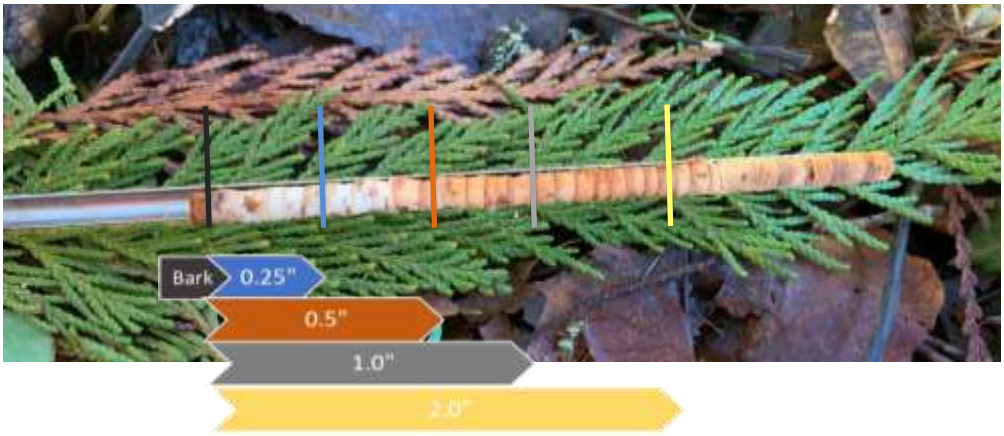

Figure 4. Example of a WRC growth increment core and the four predetermined diameter growth categories (DGC) that were counted.

Our project metrics were also adapted by University of Washington researchers for use in iNaturalist to engage citizen scientists and broaden collection efforts. We included 267 iNaturalist locations in our WRC dieback database after sorting out observations outside of OR/WA, healthy tree observations, single tree observations, and observations where the cause of mortality was known to be fire (Hulbert 2022: https://www.inaturalist.org/projects/western-redcedar-dieback-map). Some analyses include both Survey123 and iNaturalist collected data. Because we did not collect location data where only 'healthy' WRC occurred with the Survey123 app, for some analyses we compared our dieback database with locations of WRC distribution across OR/WA (Figure 5). Rasters of WRC distribution data were obtained from the Individual Species Parameter Maps (ITSP) (https://www.fs.fed.us/foresthealth/applied-sciences/mapping-reporting/indiv-tree-parameter-maps.shtml). Raster data were converted to a feature layer, and cells where WRC basal area >0 were clipped to WA and OR. As over 40,000 point locations occurred, we selected a 10% 'training subset' of distribution points from the larger dataset and included 4,365 WRC distribution points across WA/OR in our database. For some analyses we combined all data, but we also categorized our plot network into three distinct ecoregions: eastern WA (includes central and northeastern WA populations, cutoff at the Cascade Crest), western WA, and OR (Figure 5). In several analyses of environmental data we compared environments between ecoregions ('regions') and WRC status ('unhealthy/dieback' vs. 'WRC distribution'). We do not claim that all WRC distribution sites contain only healthy trees, but our goal was to define the environmental niche of our PNW dieback sites and compare with the environmental niche of the species' PNW distribution.

Extent of WRC dieback in Washington

Western redcedar dieback was observed across WA but was much more frequent in some areas. The extent of dieback ranged from a few locations observed near the WA coast and on the Olympic Peninsula, to a high concentration of locations observed along the low elevation urban corridor south of Olympia north along the Puget Sound, to many locations noted in the interior distribution in northeastern WA (Figure 5). Dieback was observed across interior northeastern WA populations, in central WA (what appear to be extensions of the westside populations over the Cascade Crest), in some locations on the Olympic Peninsula, and extensively along the urban corridor south of Olympia up to the Canada border (Figure 5). Small pockets of WRC dieback were observed in some drainages on the slopes of the western Cascades, but by far the most dieback noted was in lower elevations up the urban corridor along the Puget Sound and associated islands (Figures 5 and 6).

Extent of WRC dieback in Oregon

In Oregon, WRC dieback was concentrated in the north lower elevation Willamette Valley around the Portland tri-county area (Multnomah, Washington, and Clackamas counties) and in some drainages towards the coast and inland (Figure 5). There was very little WRC dieback noted (by either S123 or iNaturalist surveys) along the coast and the southern Cascades, even though these areas were also scouted (Figure 5). Much of the dieback was concentrated in oak-pine habitat and at lower elevations. Some of the mountain foothills contained pockets of old topkill but upon investigation of these stands, advanced stem rot was prolific. Many areas indicating WRC presence, particularly in the mid to lower part of the state contained healthy redcedar or a few scattered individuals at higher elevations.

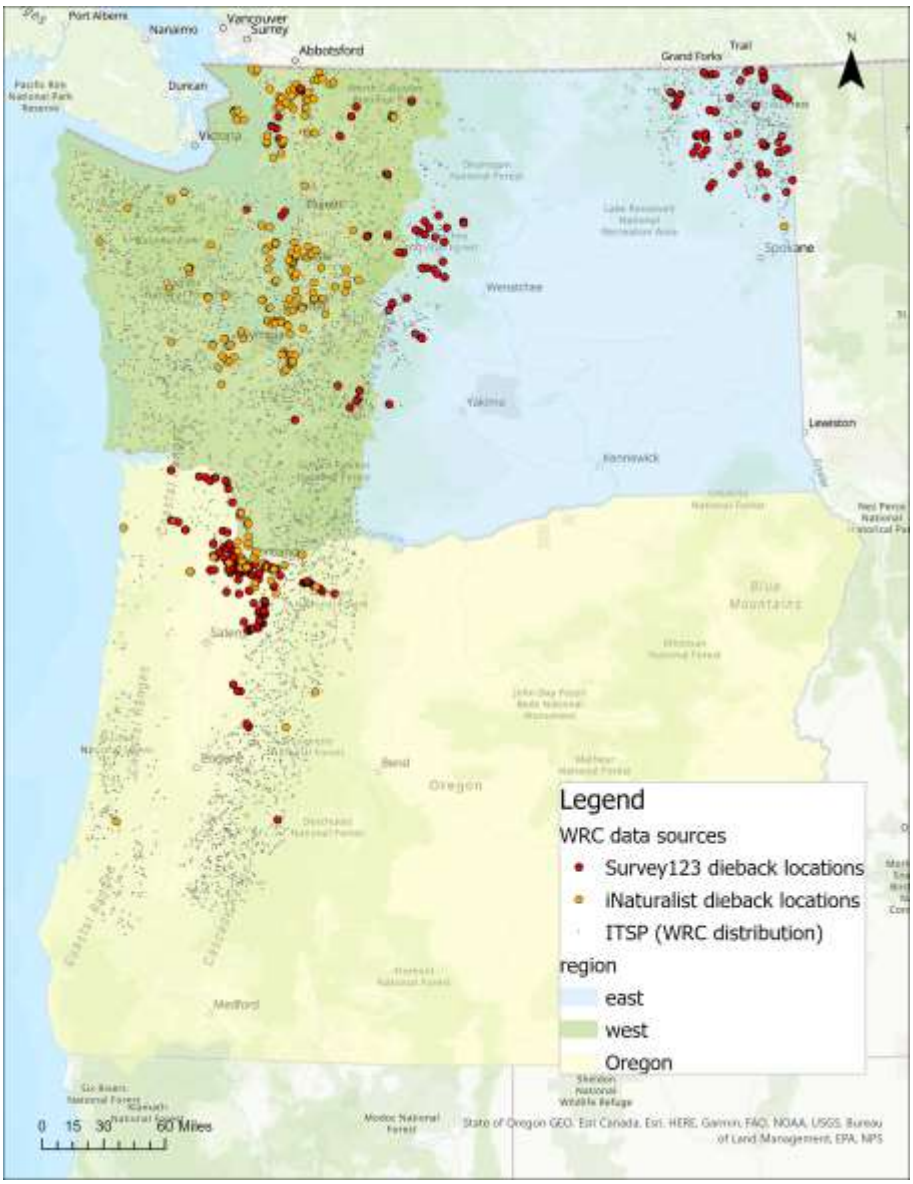

Figure 5. Data sources representing sites with ground-verified WRC dieback (S123 sites and iNaturalist sites) and data source representing WRC distribution (data from Individual Tree Species Parameter map) across Oregon and Washington. Regions are defined as western Washington (west), eastern Washington (east, separated by the Cascade Crest) and Oregon.

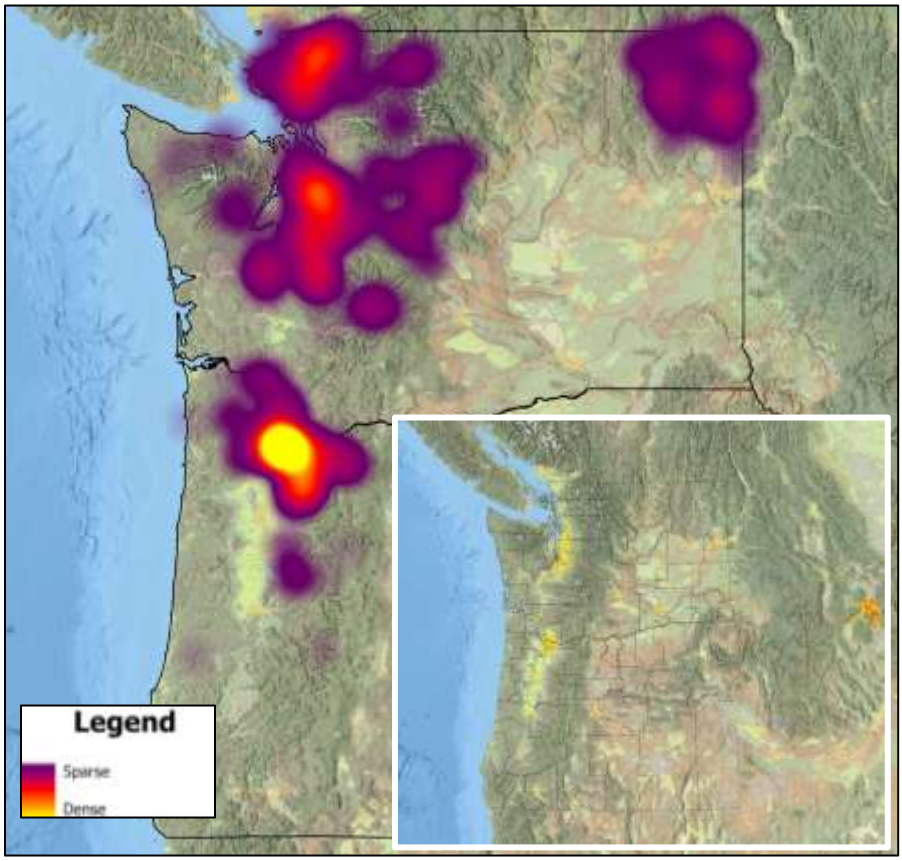

Figure 6. Heat map illustrating frequency of sites with ground verified WRC dieback indicating intensity is highest (yellow) near metropolitan areas (especially west of the Cascade crest), possibly due to a heat island effect (inset) which indicates higher temperatures (yellow) also in the metropolitan areas around Portland and Seattle. Data include all Survey123 and iNaturalist dieback locations.

Summary of data collected at western redcedar dieback sites using Survey123

Ownership type of WRC dieback sites varied by state (Table 2). In OR, most dieback was observed on small privately owned land, whereas in WA, most dieback was observed on federal land. In both OR and WA, dieback sites were most often recorded on forested land (Table 2). Average basal area (BA) per plot and average basal area of symptomatic WRC per plot varied amongst the three ecoregions with average symptomatic WRC ranging from 48 ft^2/ac in western WA to 83 ft^2/ac in eastern WA sites (Table 2). Symptomatic WRC BA generally made up 32-52% of total BA (Table 2). While we attempted to choose sites where we did not see active insect or disease activity, heartwood decay was often found during extraction of cores (Table 2 and Appendix Table A1). No single biotic damage agent was observed frequently across WRC dieback sites (Appendix Table A1). Most dieback sites occurred at lower elevations compared with the overall distribution, although this result was most pronounced in OR and western WA (Figure 7). While we expected most dieback sites to fall on southerly aspects, dieback sites in OR commonly occurred at sites with no slope, while dieback sites in WA were most often found on westerly facing slopes (Figure 8). Slope position varied greatly by region and even within region (Figure 9). In OR, most dieback sites were recorded on no slope or backslopes; in eastern WA toeslopes and backslopes were common; and in western WA backslopes and valley bottoms were most common (Figure 9). Slope position was determined on a smaller stand-level scale versus a larger landscape-level scale to more accurately depict influence on microclimate in the immediate area. The dominant

overstory tree species found at dieback sites in all three regions was WRC followed by Douglas-fir (Table 3).

Table 2. Summary statistics of ground-verified sites with WRC dieback using Survey123 collected points.

		Region		
		OR	Eastern WA	Western WA
Ownership Type (% Plot)	Federal	3.4%	62.8%	43.7%
	State	1.1%	11.5%	12.7%
	Industrial Private	3.9%	8.8%	4.2%
	Small Private	64.8%	13.3%	22.5%
	Local	26.3%	0.9%	2.8%
	Other	0.6%	2.7%	14.1%
Site Type (% Plot)	Forest	57.2%	98.3%	91.5%
	Urban Natural	37.2%	1.7%	1.4%
	Urban Landscaped	5.6%	0.0%	7.0%
Basal Area (ft^2/ acre)	Average/ Plot	130.4	154.7	164.7
	Avg. Symptomatic WRC/ Plot	61.6	83.4	47.6
	Avg. % of plot with symptomatic WRC	50.1%	52.5%	33.0%
Insects & Disease (including decay) Presence	No	94%	38%	59%
	Yes	6%	62%	41%

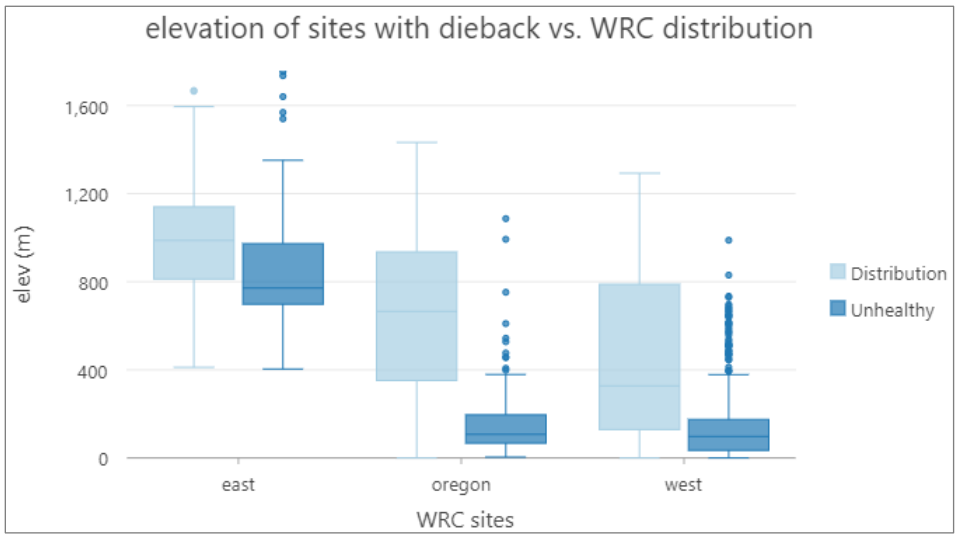

Figure 7. Sites with ground verified WRC dieback generally occupied lower elevation areas when compared to the WRC distribution in each region. WRC distribution and dieback in central/eastern Washington ('east') occurred at notably higher elevations relative to populations in Oregon and western Washington. Boxes represent the 1st and 3rd quartiles of the data, box error bars represent minimum and maximum, and the median is defined as a line in the box center. Dots are considered outliers.

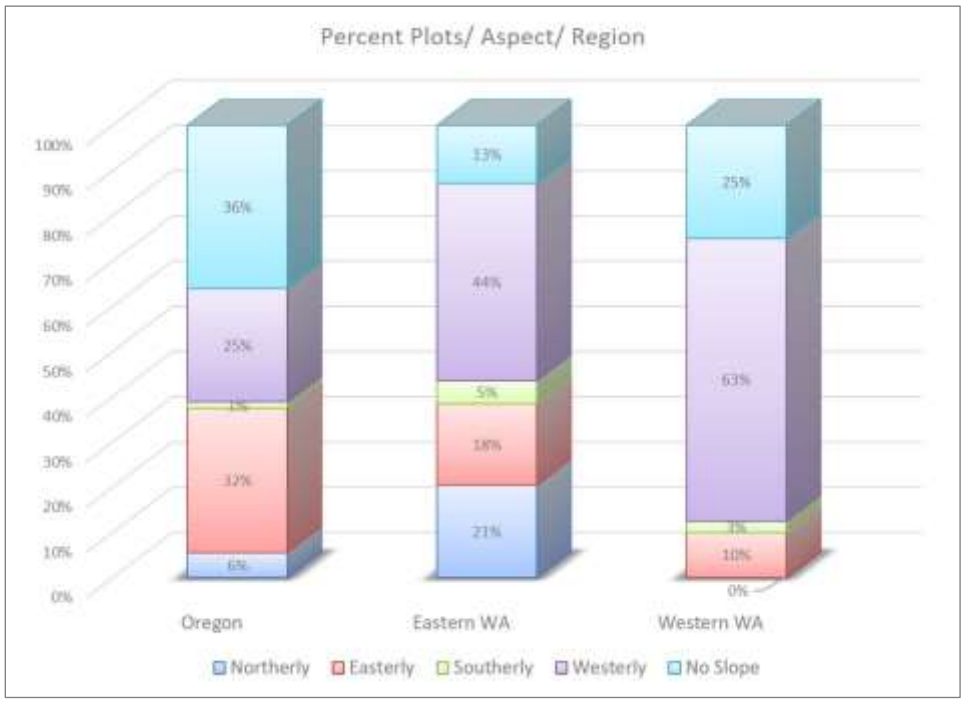

Figure 8. Percentage of ground verified Survey123 collected dieback locations in various aspect categories. All slopes with a western orientation (i.e. NW, SW) were categorized as 'westerly' and all slopes with an eastern orientation (i.e. NE, SE) were categorized as 'easterly' and north and south remained the same (http://meted.ucar.edu/). Westerly slopes were most dominant in both eastern and western Washington sites, but 'no slope' was the dominant aspect category across Oregon.

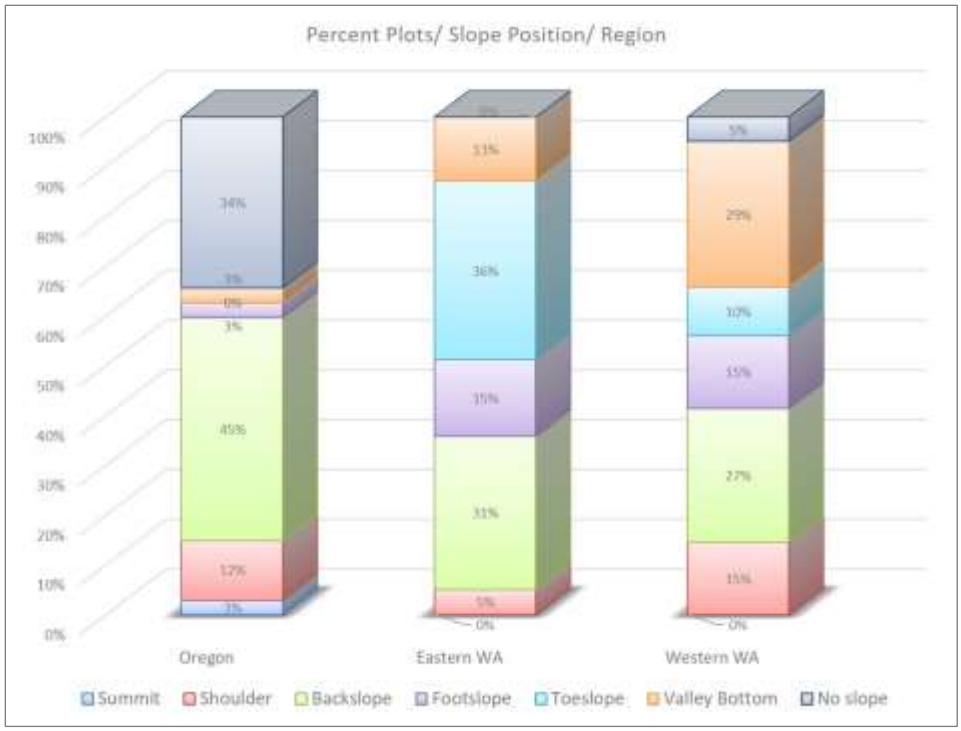

Figure 9. Percentage of ground verified Survey123 collected dieback locations in various slope positions by region. Backslope and toeslope were the most common slope positions in both Oregon and eastern Washington. More valley bottom sites were recorded in western Washington compared to the other regions.

Table 3. Frequencies of dominant overstory tree species associated with ground verified sites with WRC dieback collected using Survey123.

	Dominant Overstory Species									
Location	Western Redcedar	Douglas-fir	Bigleaf Maple	Red alder	Oregon White Oak	Western Hemlock	Grand fir	Mountain Hemlock	Subalpine fir	Western larch
Oregon	46	9	7	2	3	0	0	0	0	0
Eastern WA	25	10	0	0	0	1	1	0	1	1
Western WA	14	11	8	3	0	2	0	1	0	0
Total	**85**	**30**	**15**	**5**	**3**	**3**	**1**	**1**	**1**	**1**

Summary of monitor tree data collected at western redcedar dieback sites using Survey123

The average DBH and average number of growth rings in each DGC was not different among ecoregions (Table 4). Across all three regions, the majority of monitor trees fell into the 100 or 300 year age estimate categories and were in the codominant canopy position (Table 4, protocols highly suggested selecting monitor trees of codominant or dominant crown class, age estimations from Van Pelt 2008). Of the crown symptoms of dieback observed, crown thinning was the most common symptom observed, followed by branch dieback (Figure 10). We only chose live symptomatic monitor trees, so we did not record mortality. Future surveys should include the presence of WRC mortality at the site as a site notation, and possibly try to capture the density of dead WRC.

Table 4. Summaries of monitor tree data collected at western redcedar dieback sites using Survey123

		Region		
		OR	Eastern WA	Western WA
Average diameter at breast height (DBH) of monitor trees	n	67	38	40
	Average DBH	29.4	25.0	32.7
	Range	2.2-56.5	9.9-82.0	10.4-80.0
Average number of annual growth rings in each DGC	n	64	30	8
	0.25"	3.4	6.6	5.0
	0.5"	6.3	12.2	8.6
	1.0"	11.1	22.1	14.0
	2.0"	20.6	39.1	26.2
	Range (2.0")	7.0-58.0	17.0-110.0	18.0-37.0
Frequencies of monitor trees within estimated age categories (Van Pelt 2008)	50	17	1	7
	100	28	21	23
	300	20	16	10
	500	2	1	0
	1500	0	0	0
Frequencies of monitor trees within crown classification categories	Suppressed	1	0	0
	Intermediate	6	4	3
	Codominate	39	28	29
	Dominant	20	6	7

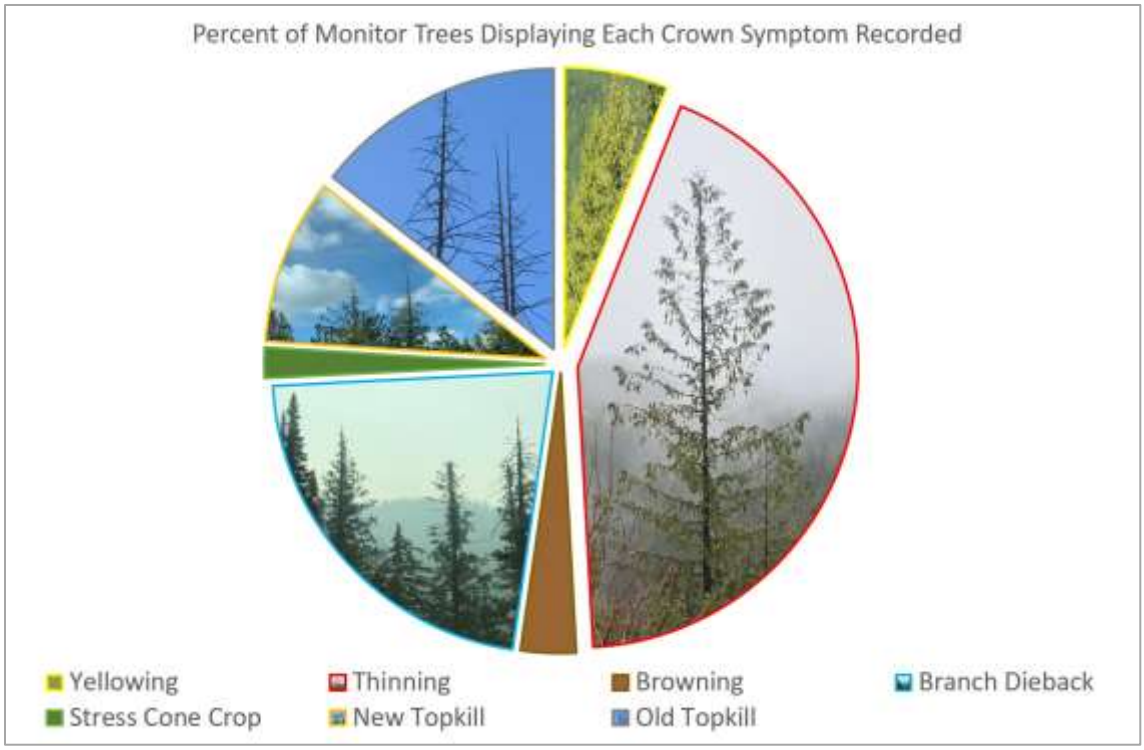

Figure 10. Proportion of crown symptom of dieback in all ground-verified Survey123 sites with WRC dieback. Most sites had multiple crown symptoms recorded. Thinning crowns were by far the most common symptoms observed. Note: We did not select monitor trees with mortality, so mortality was not recorded.

Statistically significant relationships between site factors and dieback/growth

In our plots across our combined ecoregions in WA and OR we found that (see Table 5):

- Monitor trees with larger DBH tended to be in stands with lower basal area of unhealthy WRC *(potential interpretation: larger diameter trees are more vigorous and can better overcome site or climate stress)*
- Stands with higher basal area tended to also have a higher proportion of symptomatic WRC basal area as well as a slower growth within each DGC *(potential interpretation: more competition may result in more WRC with dieback that gain less diameter growth over time)*
- Intermediate crown classes exhibited the fastest growth within the 0.5" and 1.0" DGCs *(potential interpretation: trees growing in the intermediate crown class benefit from more shading and have fewer water needs than larger trees and thus have benefitted during some periods when it comes to diameter growth rate)*
- Trees growing on toe slopes yielded the highest number of rings (significant only in most recent 0.25" of diameter growth) *(this result was most pronounced in eastern WA, and we do not have an adequate hypothesis to propose, but suggest a larger sample size to test this interaction).*
- NE slopes contained the most trees with high dieback ratings and south slopes contained the most trees with a medium rating *(potential interpretation: these contrary results indicate aspect may have been evaluated at too small of a scale (i.e. using local micro-topography relative to a larger macro- landscape aspect). We did struggle with aligning observations of aspect and slope*

position for this species that often occurs in small drainages, ephemeral streambeds, shady pockets, along edges of waterways, etc. However, we downloaded and attached aspect data derived from digital elevation models and did not observe any patterns at dieback sites vs. distribution sites with those data either.)

Table 5. Significant interactions from ANOVA analyses (pairwise comparisons made with student's t-tests for regressions and Pearson's for Chi^2) across all regions

Predictor variable	Response variable	All ecoregions combined
DBH	Unhealthy WRC basal area	Negative correlation
Basal area	Unhealthy WRC basal area	Positive correlation
Basal area Crown class	No. rings in 0.25"	Positive correlation
	No. rings in 0.5"	Positive correlation
	No. rings in 1.0"	Positive correlation
	No. rings in 2.0"	Positive correlation
	No. rings in 0.5"	all other crown classes <intermediate
Crown class Slope position	No. rings in 1.0"	all other crown classes <intermediate
	No. rings in 0.25"	Toe slope significantly highest number of rings
Aspect	Dieback rating	Highest rating in N=SW<W<no slope<NE Medium rating in no slope<all aspects except S<S

Exploratory relationships between climate/weather data and WRC dieback

We hypothesized that abiotic factors were associated with WRC dieback across the PNW. To explore relationships of various weather/climate variables between dieback locations and the OR/WA distribution of WRC, we downloaded 30-year normal data (for the period 1991-2020) and yearly data from 2015 from ClimateNA v7.20 (Wang et al. 2016) for all 4,962 locations (most locations representing the WRC distribution across WA and OR and the remaining locations with ground verified WRC dieback) (Figure 5). A small subset of locations had null values for some climate/weather variables and were excluded from analyses. We then explored distributions of climate/weather variables such as precipitation, temperature, and other calculated variables between the distribution points and dieback points.

Because we hypothesized that dieback sites may occur at sites with less average precipitation or higher average/seasonal temperatures, we explored and compared 30year climate normal data by region and WRC status (distribution vs. unhealthy points). We also hypothesized that when a severe drought year occurred, sites with dieback may occur in even hotter, drier sites than the rest of the distribution, so we downloaded data for an extremely dry year in both states (2015) and explored precipitation, temperature, vapor pressure deficit, and many derived variables by region and WRC status (Figures 11 and 12). We hypothesized that early spring weather may be important for WRC growth and health, especially in westside systems. Sites with WRC dieback ('unhealthy' WRC status) generally had lower long-term April, May, and June precipitation and the ranges were smaller compared to the WRC distribution ('distribution' WRC status), but 2015 medians and variance were closer between distribution and dieback sites (Figure 11). Long-term and 2015 maximum temperature were both generally higher (and variance smaller) in sites where WRC dieback occurred compared to sites across the OR/WA WRC distribution.

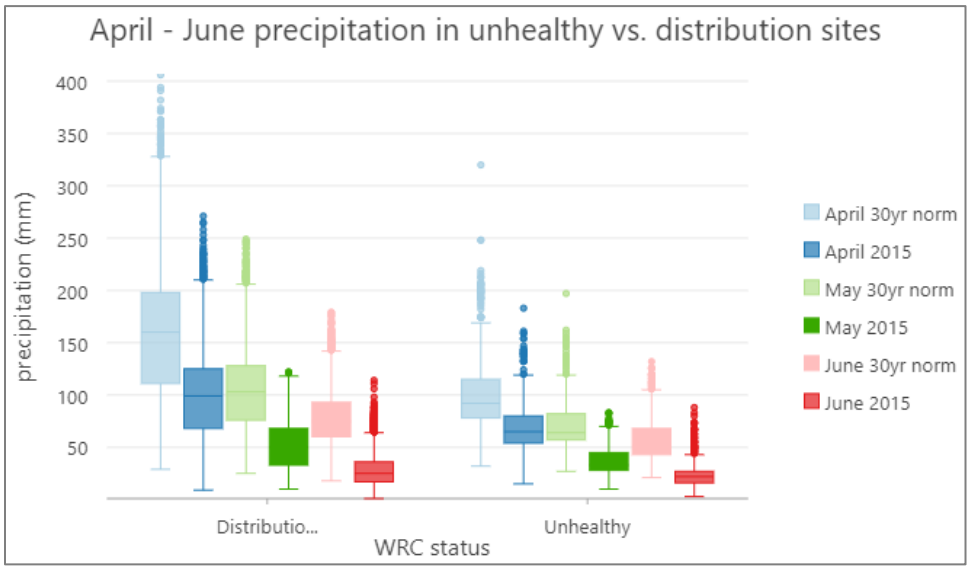

Figure 11. Distribution of April, May, and June precipitation (mm) 30year normals (1990-2020) and the same months of precipitation in 2015 (a drought year in both Oregon and Washington, see Figure 2) at WRC 'distribution' sites compared to sites with ground verified WRC dieback ('unhealthy'). Boxes represent the 1st and 3rd quartiles of the data, box error bars represent minimum and maximum, and the median is defined as a line in the box center. Dots are considered outliers.

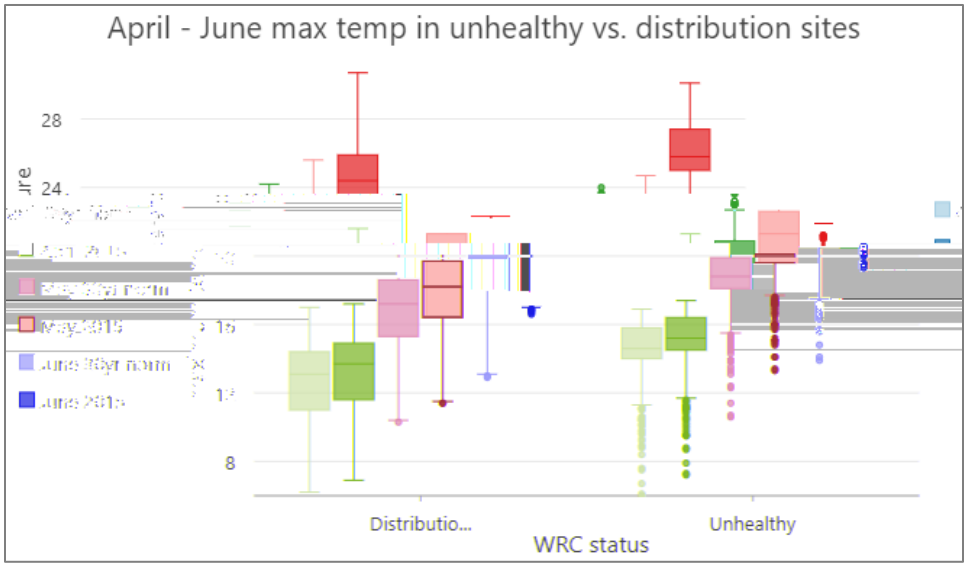

Figure 12. Distribution of April, May, and June maximum temperature 30year normal (1990-2020) and the same months of temperature in 2015 (a drought year in both Oregon and Washington, see Figure 2) at WRC 'distribution' sites compared to sites with ground verified WRC dieback ('unhealthy'). Boxes represent the 1st and 3rd quartiles of the data, box error bars represent minimum and maximum, and the median is defined as a line in the box center. Dots are considered outliers.

To narrow down the list of potential climate/weather variables associated with WRC dieback, we explored data using categorical and regression tree (CART) models. CART models are useful to explore data structure and develop easy to visualize decision rules for predicting categorical variables such as ours (Kabacoff 2017). CART models can be used for classification or regression predictive modeling problems. We used the classification method to help predict occurrence of either 'distribution' or 'unhealthy' WRC points, where unhealthy points were ground-verified locations with dieback and distribution points were from the Individual Tree Species Parameter dataset (Figure 5). CART models are essentially a string of if-else statements, where the nodes are split into subnodes on the basis of a threshold value of an attribute (in our case we included a suite of seasonal temperature, precipitation, and calculated variables as potential predictive variables) (see Appendix Table A2 for full list of variables). We viewed full models and then pruned each tree to avoid overfitting the data by viewing graphs of cross-validated error results and complexity parameters and selecting the number of nodes that minimized the cross-validated error and complexity parameter value (Kabacoff 2017, Milborrow 2020). We ran two separate models, one for westside locations (combining OR and western WA into one model) (Figure 13) and one for eastside locations (Figure 16).

Westside (western Washington and Oregon) CART model

The complexity parameter (cp) of 0.029 minimized error (relative error = 0.69557) and was associated with five nodes in the full westside tree, so the final westside model was pruned to five nodes using the cp value of 0.029 (Table 6, Figure 13). The pruned westside CART model included the climate predictor variables of precipitation as snow from March-May (PAS_sp), mean warmest month temperature (MWMT), mean seasonal precipitation (MSP), and fall Hogg's climate moisture index from September-November (CMI_at) as predictors (Table 6). Hogg's climate moisture index (CMI) is described as the difference between annual precipitation and potential evapotranspiration (PET) – the potential loss of water vapor from a landscape covered by vegetation (Hogg et al. 1997). Higher CMI values indicate wet

or moist conditions and lower CMI values indicate drier conditions (Hogg et al. 1997). Each node at the bottom of the westside CART model shows three items: 1) the predicted class (distribution or unhealthy), the predicted probability of being unhealthy, 3) the percentage of all observations in the node (Figure 13).

The first node to split data in the westside model was precipitation as snow in spring (March - May, mm). A very low threshold of >3 mm predicted 90.1% of all observations as 'distribution', with a low probability (0.066) of these observations being misclassified as 'unhealthy' (Figure 13). All predicted unhealthy locations fell to the right side of the tree below the threshold of PAS_sp < 3 mm (Figure 13). The next node for splitting was mean warmest month temperature (°C) and the threshold for a split was 19.9 °C. Most of the remaining observations fell below this threshold and needed further splitting, but 3.3% of all observations were classified as 'unhealthy' at this split when MTWM was above 19.9 °C with a high probability of being classified correctly as unhealthy (0.923, Figure 13). The relationship between the first node (spring precipitation as snow) and two other node variables (mean temperature in the warmest month and autumn climate moisture index) are shown in Figure 14A and B, respectively. Most 'unhealthy' dieback points clustered below the spring PAS threshold of 3 mm and at the higher end of the mean warmest month temperature (Figure 14A) and the lower end of the autumn climate moisture index (Figure 14B).

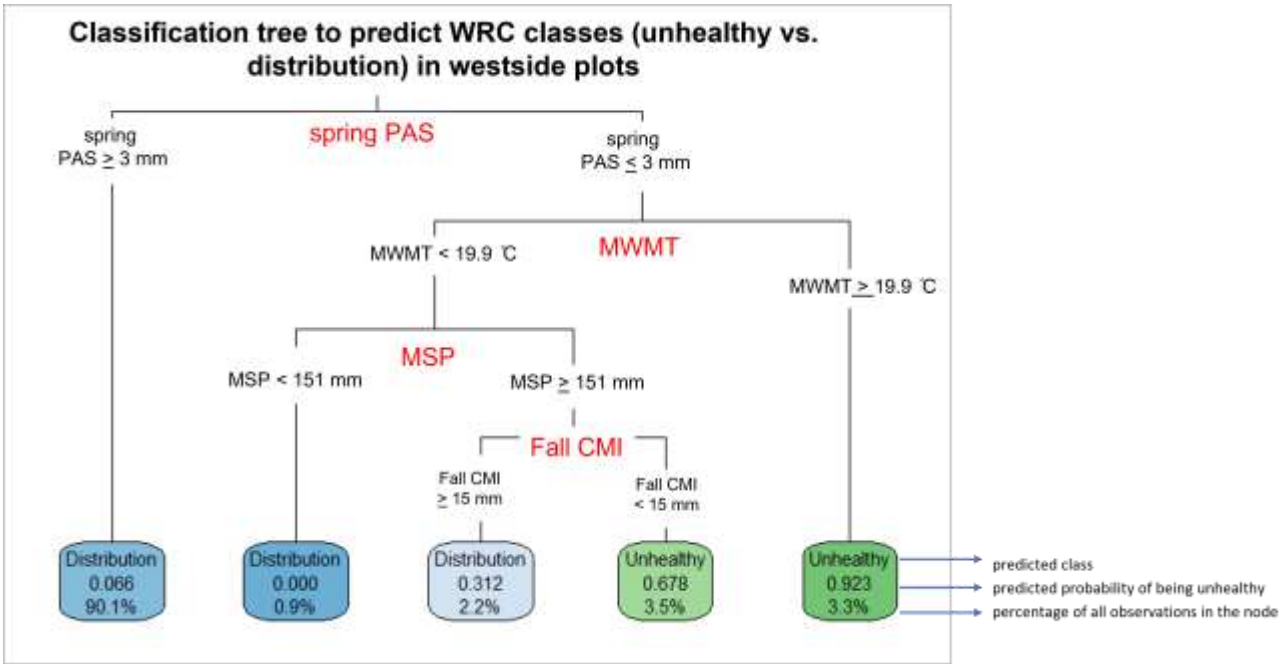

*Figure 13. Classification tree for westside plots (western Oregon and western Washington). The full selection of climate predictor variables is available in Appendix Table A2. Each node at the bottom of the westside CART model shows three items: 1) the predicted class (distribution or unhealthy), the predicted probability of being unhealthy, 3) the percentage of all observations in the node. The complexity parameter (cp) of 0.029 minimized error (0.69557 error) and was associated with five nodes in the full westside tree, so the final westside model was pruned to five nodes using the cp value of 0.029. The tree had a misclassification rate of 8.4% in cross-validation (calculated as root node error * xerror * 100% = 0.12115 * 0.69557 *100) (following methods in Ma 2014).*

Table 6. Variables selected in westside cart model, sample size, and root node error

Westside CART model		
Variable	Description	Node 'split' value
PAS_sp	Spring (March - May) precipitation as snow (mm)	3
MWMT	Mean warmest month temperature (°C)	19.9
MSP	May to September precipitation (mm)	151
CMI_at	Autumn (Sept-Nov) Hogg's climate moisture index (mm)	15
n= 4284		
Root node error: 519/4284 = 0.12115		

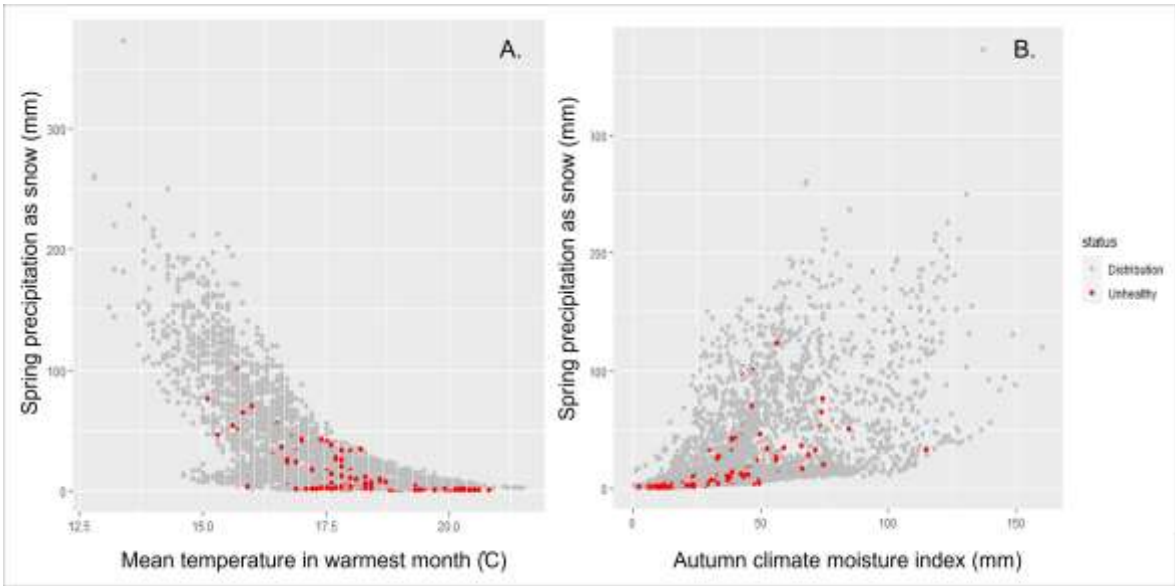

Figure 14A-B. Variation and grouping of WRC status for first and second predictor variables (nodes) in westside CART model (PNAS_sp and MWMT). Most of the unhealthy points fell below the PAS_sp value of 3 mm (first split in pruned CART model predicted all unhealthy points fall under PAS_sp < 3 mm) and also at the higher end of the mean warmest month temperature (CART model predicted split at 19.9 degrees C). A proportion of the unhealthy points are below the predicted CMI_at threshold of < 15 (last node split).

When the full dataset was mapped and classified according to a single climate threshold of spring precipitation as snow (PAS_sp) above or below 3mm, the unhealthy data are predominately in the low elevation urban corridor from the Portland/Multnomah county area up north to Seattle area, along the Puget Sound and coastal areas on both sides of the Sound (including islands and the northeastern tip of the Olympic Peninsula) (Figure 15). When we overlay the ground verified locations with WRC dieback on top of these predictions, there was some agreement that many verified locations of dieback occur in this area (Figure 15). While data do not align perfectly, we feel the spring precipitation as snow looks to be a fairly predictive variable to explain where dieback is most likely to occur in westside systems (see misclassification rate of CART model) and could be used in further exploratory or predictive models. In WA, the first node of the CART model did not appear to accurately predict sites along western slopes of

the Cascades or further west on the Olympic Peninsula where dieback has been observed (Figure 15). The model did predict dieback along the north and northeast side of the Peninsula, where there is some rainshadow effects. In OR, the model appears to misclassify the location and/or density of redcedar of many currently healthy sites in southern OR (coastal and the interior) as sites with dieback. Many of those sites were scouted for dieback, and either a low incidence of redcedar was observed, dieback was not present or spare, or dieback was present only as old topkill (remaining crown still green) and extensive stem decay was evident as a confounding factor.

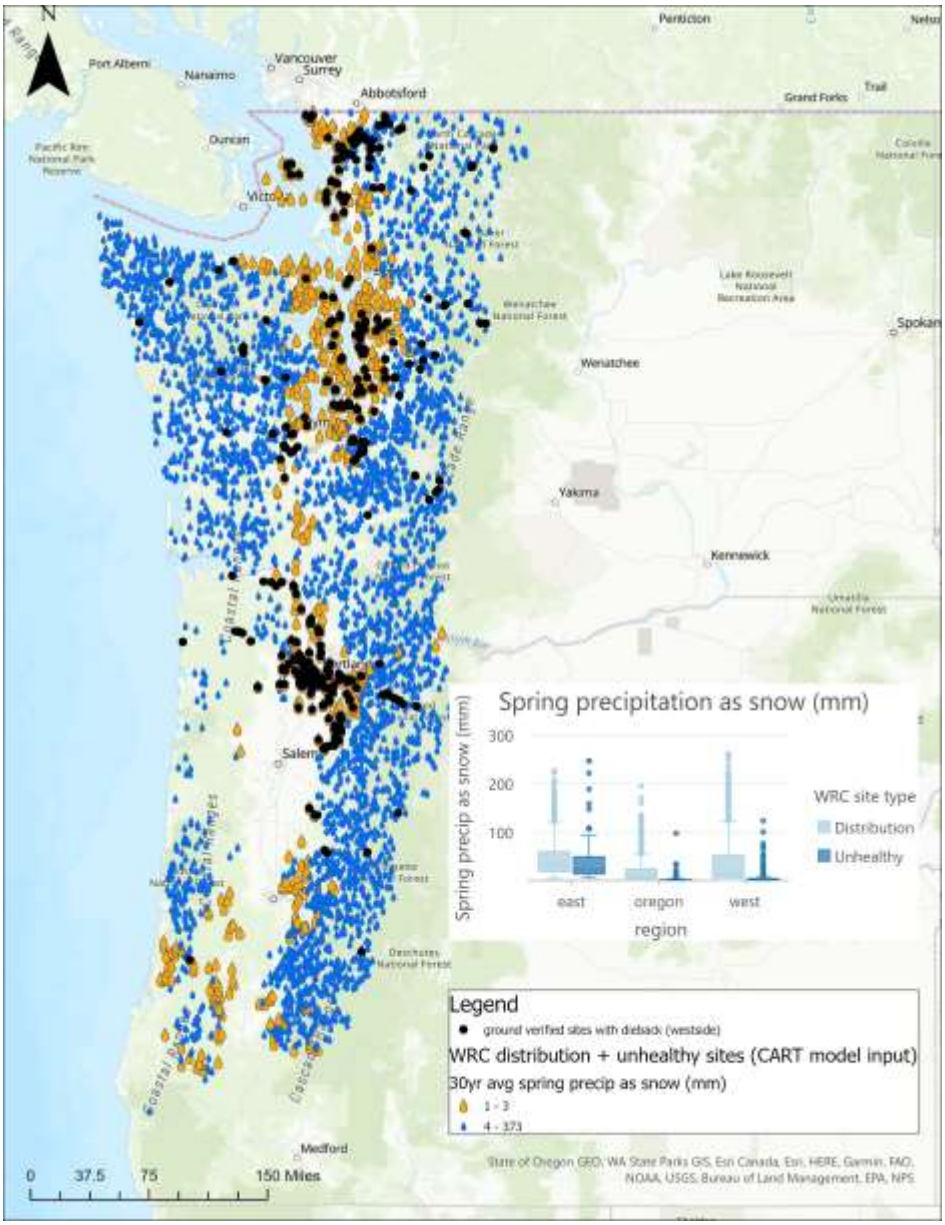

Figure 15. All WRC database locations separated by first predictive node (spring precipitation as snow > 3) in westside CART model (blue and orange droplets represent above and below the first node threshold of PAS_spring, respectively). Network of ground verified WRC dieback locations overlaid on top (data sources = Survey123 and iNaturalist WRC dieback projects). Inset graph: spring PAS medians/quartiles separated by region and WRC status.

Eastside (central and eastern Washington) CART model

The complexity parameter (cp) of 0.031 minimized error (relative error = 1.0256 error) and was associated with five nodes in the full eastside tree, so the final eastside model was pruned to five nodes using the cp value of 0.031. The tree had a misclassification rate of 17.2% in cross-validation (calculated as root node error * xerror * 100% = 0.16318 * 1.0256 *100) (following methods in Ma 2014). The pruned eastside CART model included the climate predictor variables of summer (June-August) Hogg's climate moisture index, extreme minimum temperature over 30 years (EMT), Hargreaves reference evaporation (mm, Eref), and precipitation as snow as predictors (PAS, Table 7, Figure 16). The Climate Moisture Index (CMI) is described as the difference between annual precipitation and potential evapotranspiration (PET) – the potential loss of water vapor from a landscape covered by vegetation (Hogg et al. 1997). Higher CMI values indicate wet or moist conditions and lower CMI values indicate drier conditions (Hogg et al. 1997). Each node at the bottom of the eastside CART model shows three items: 1) the predicted class (distribution or unhealthy), the predicted probability of being unhealthy, 3) the percentage of all observations in the node (Figure 16).

The first node to split data in the eastside model was summer (June-August) Hogg's climate moisture index (Figure 16). A low threshold of -30.9 mm split data, but all data needed at least one more split. The extreme minimum temperature predictor of -27.2 split 2.9% of the observations as 'unhealthy' (probability of 0.714) and 2.5% of the data as 'distribution' (Figure 16). Most observations were split using autumn Eref (following the summer CMI split) of less than 128 mm (57.5% of observations were predicted as 'distribution') (Figure 16). All data with autumn Eref > 129 needed the additional variable PAS to split data at 312 mm, and the remaining 'unhealthy' observations were associated with more than 312 mm precipitation as snow (Figure 16). The relationship between the first node (summer CMI) and two other node variables (EMT and autumn Eref) are shown in Figure 17A-B. Compared to westside models, the eastside 'unhealthy' points seemed distributed more evenly throughout the WRC 'distribution'. There is some visible grouping of unhealthy points at the high end of the autumn Eref and low end of summer CMI. An additional note about the eastside model is that when site attributes were included as potential predictor variables the first node selected to split data was elevation, where more 'unhealthy' sites occurred at lower elevations. We ultimately decided to limit potential predictor variables to only climate variables in both models and did not include elevation, aspect, etc. in any potential models, but they could potentially improve the eastside model.

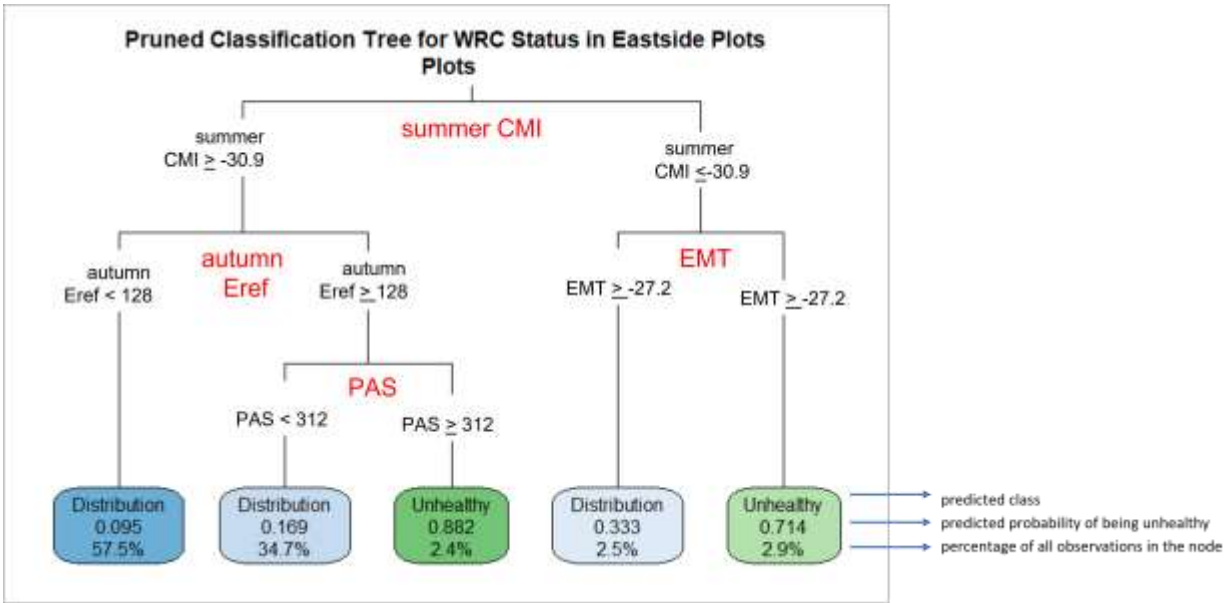

*Figure 16. Classification tree for eastside plots (central and eastern WA). The full selection of climate predictor variables is available in Appendix Table A2. Each node at the bottom of the eastside CART model shows three items: 1) the predicted class (distribution or unhealthy), the predicted probability of being unhealthy, 3) the percentage of all observations in the node. The complexity parameter (cp) of 0.031 minimized error (1.0256 error) and was associated with five nodes in the full eastside tree, so the final eastside model was pruned to five nodes using the cp value of 0.031. The tree had a misclassification rate of 17.2% in cross-validation (calculated as root node error * xerror * 100% = 0.16318 * 1.0256 *100) (following methods in Ma 2014).*

Table 7. Variables selected in eastside cart model, sample size, and root node error

Eastside CART model		
Variable	Description	Node 'split' value
CMI_sm	Summer (June-Aug) Hogg's climate moisture index (mm)	30.9
EMT	Extreme minimum temperature over 30 years	-27.2
Eref	Hargreaves reference evaporation (mm)	128
PAS	Precipitation as snow (mm). For individual years, it covers the period between August in the previous year and July in the current year	312
n= 717		
Root node error: 117/717 = 0.16318		

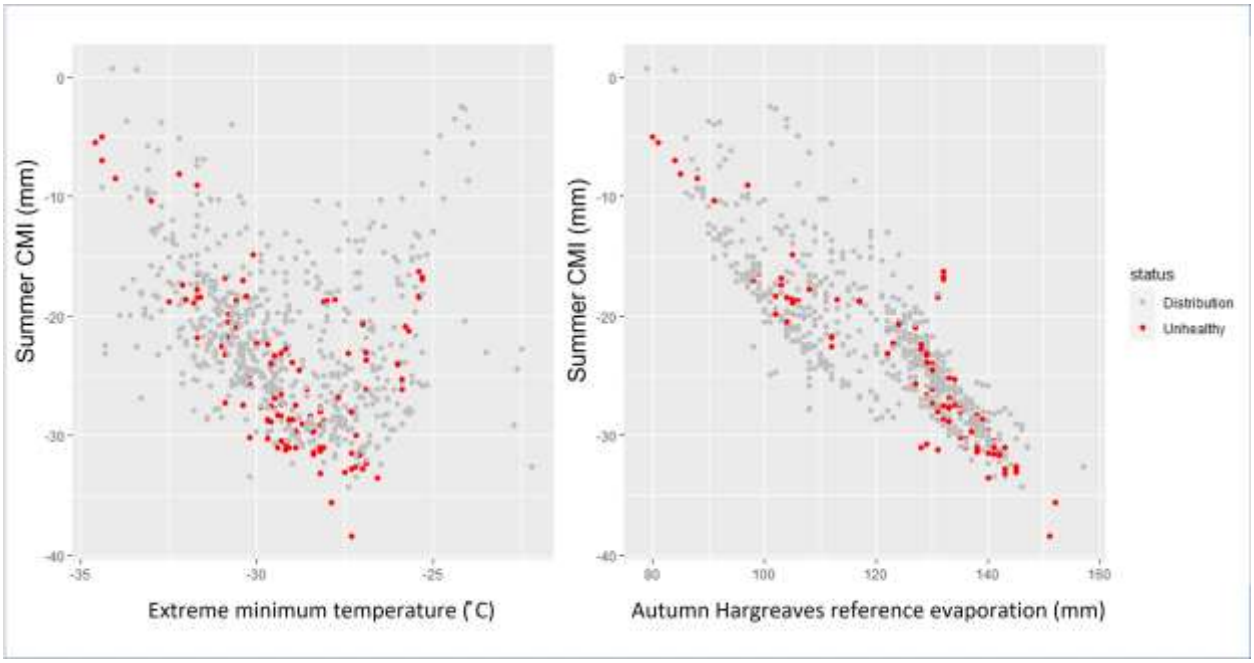

Figure 17A-B. Variation and grouping of WRC status for first, second, and third predictor variables (nodes) in eastside CART model (CMI_sm, EMT, and Eref_at)). Both distribution and unhealthy datapoints are spread throughout the distribution of each variable, although unhealthy points do appear visibly clustered towards the low end of summer CMI and the high end of autumn evaporation.

When the full dataset was mapped and classified according to a single climate threshold of summer climate moisture index (CMI_sm) above or below -30.9mm, sites predicted as unhealthy were apparent in both central and northeastern WA, generally in areas towards the edges of the WRC distribution (Figure 18). When we overlay the ground verified locations of WRC dieback on top of these predictions, there was some agreement where verified locations of dieback occurred, especially in north-central WA and some of the most southern locations in northeastern WA (Figure 18). The eastside model had a higher misclassification rate and did not appear as useful as the westside when known locations of dieback were aligned. Lower summer climate moisture index as the first node to split data illustrates that WRC dieback is occurring in drier, hotter locations in eastern WA, and including climate moisture index may be useful in further exploratory or predictive models. Dieback sites in the very northeastern WA locations (generally east of the Pend Oreille River and higher elevations) were not accurately predicted (Figure 18).

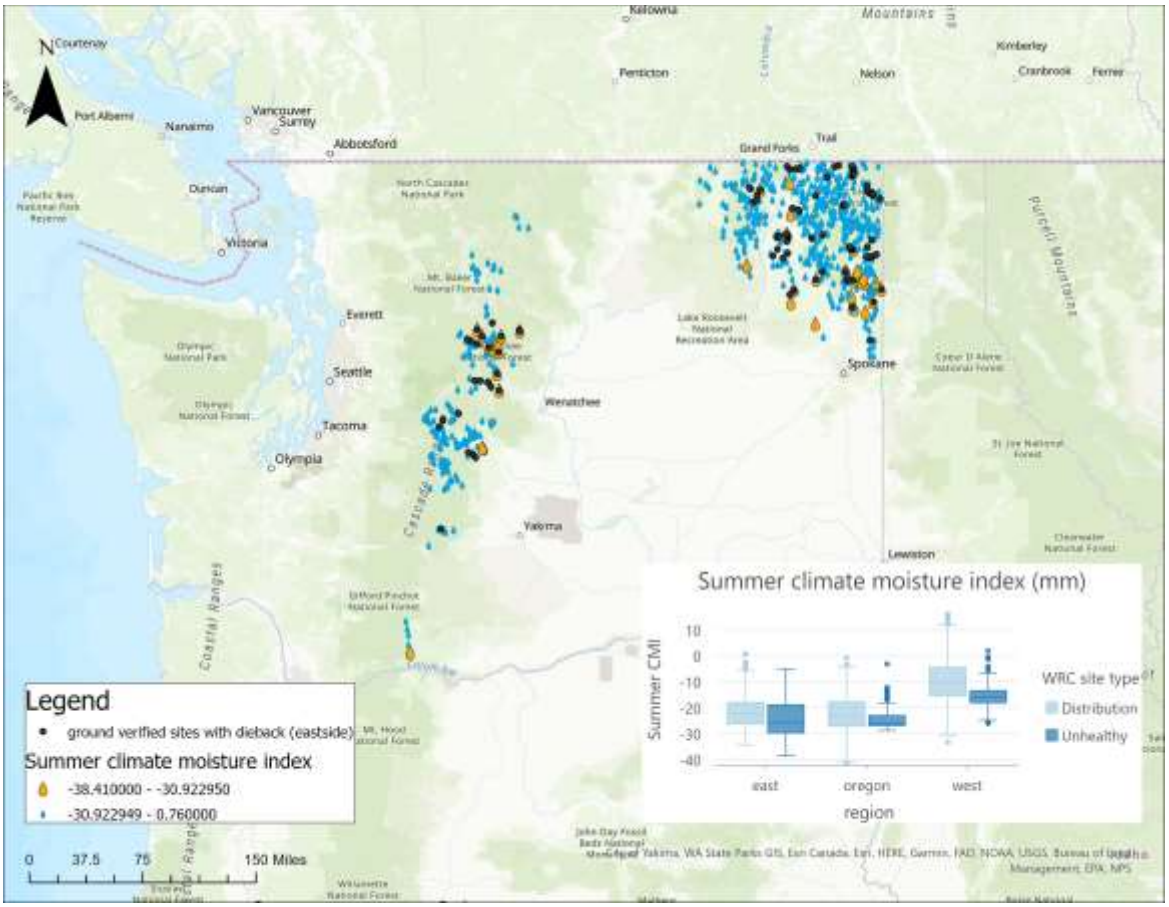

Figure 18. All WRC database locations separated by first predictive node (summer Hogg's climate moisture index < -30.9mm) in eastside CART model (blue and orange droplets represent below and above the cutoff of summer CMI, respectively). Eastside ground verified WRC dieback locations overlaid on top (data sources Survey123 and iNaturalist WRC dieback projects). Inset map: Summer CMI values separated by region and WRC status.

Conclusions

- WRC dieback was observed across the PNW distribution of WRC, with the exceptions of coastal and higher elevation mountainous regions of OR
- Frequency of WRC dieback locations were highest in low elevation, urban corridors in western WA and northwestern OR
- The most common symptom of WRC dieback was thinning crowns, followed by branch dieback
- No site factors were associated with higher severity of individual tree crown dieback or transparency
- At sites with dieback, symptomatic WRC made up approximately 30-50% of the total basal area
- No biotic damage agent was found associated with WRC dieback across the region
- More WRC dieback sites were observed at lower elevations compared to the WRC distribution across the PNW
- More dieback sites were observed on westerly slopes in WA, and areas with no slope in OR
- Dieback sites were not strongly associated with any one slope position

- In westside systems (western WA and OR), low spring precipitation as snow was the first chosen predictor variable from a suite of climate variables, and appeared to be a fairly strong predictor variable separating sites with dieback from the WRC distribution
- In eastside systems (central and eastern WA), low summer climate moisture index was the first chosen predictor variable from a suite of climate variables, but was not a strong predictor variable separating sites with dieback from the WRC distribution

Proposed future directions

- We have identified specific sites that are conducive to further study, based on presence of symptoms across larger areas, ease of access and landowner permission. At a subset of these sites we recommend (and will continue to develop collaborations with specialists to investigate):
    - Tree dissections (e.g. rings at various stem heights, close inspection of dead tops), in-depth root investigations (e.g. depth and area of roots)
    - More thorough, local investigations into soil type, texture, drainage, etc. at sites with WRC dieback. Note: We downloaded and attached course-scale soils information to our locations but did not visibly note any obvious patterns of sites with dieback to investigate further. We investigated some available comprehensive soils variables available from FHAAST, such as Drainage Index (see Figure A1 in Appendix) and Productivity Index, but did not see large differences between sites with dieback and sites that represented the entire WRC distribution (Appendix Figure A1).
    - Investigate physiology in various canopy positions (e.g. sun vs. shade, top vs. lower crown)
    - Use dendrochronology (tree cores) to determine if reduced growth or dieback severity were associated with drought years between symptomatic trees and nearby healthy trees (in progress by Adams/Moffat labs, Washington State University)
    - Note: PIs have committed to revisit a subset of sites to monitor progression of symptoms
    - Note: PIs will keep Survey123 open and updated and continue to collect location data

- More in-depth pattern analyses of climate data, site index, microtopography, and other variables such as the effect of heat islands that may influence WRC dieback occurrence from tree to tree.
- Continue scouting dieback locations across areas that were not adequately sampled within the timeline of this project (i.e. Olympic Peninsula, Idaho, British Columbia)

APPENDIX

Appendix Table A1. Biotic damage agent presence (when possible, we avoided selecting monitoring trees with obvious insect or disease signs and symptoms that may confound our search for the mortality causal agent):

	OR	Eastern WA	Western WA
Drought Scorch	0	0	1
Heart Rot	2	12	7
Keithia Blight	0	0	1
Mechanical Wound	1	0	9
Old Unidentified Basal Canker	1	0	0
Phloeosinus spp.	0	0	2
Root Disease	0	1	1*
Woodborers	0	0	3
Woodpecker	0	1	0

*Root pathogen identified as *Armillaria sinapina*, first report on dying *Thuja plicata* host in Washington (pers. comm. Mee-Sook Kim, PNW Research, Corvallis, OR).

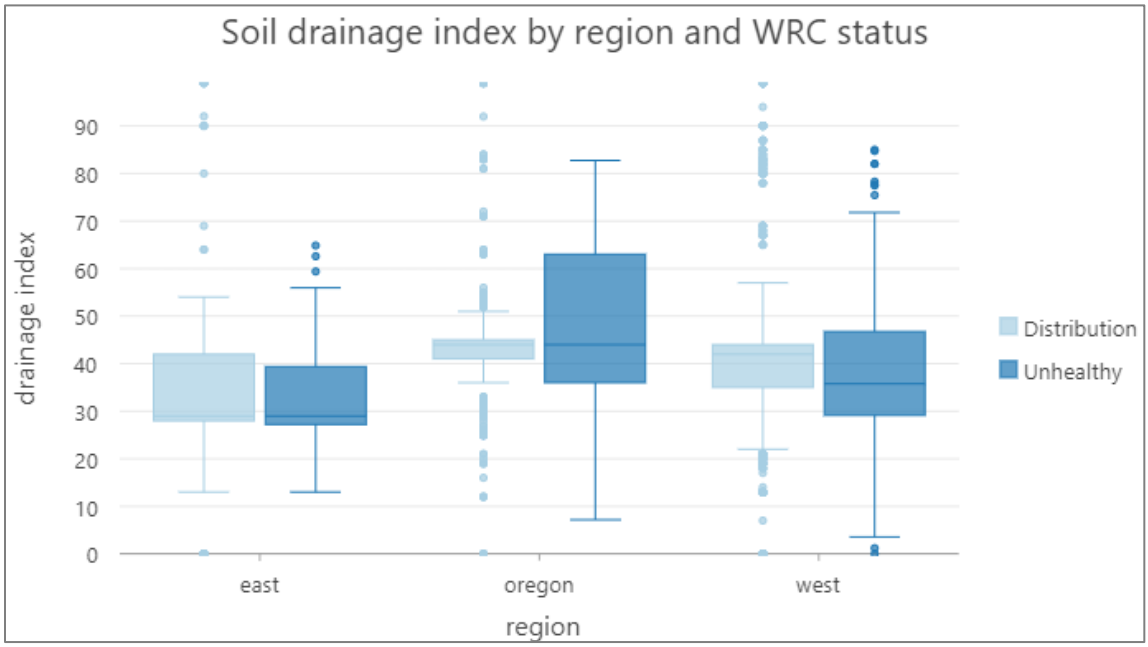

Appendix Figure A1. Soil drainage index. The Drainage Index (DI), originally named the "natural soil wetness index" (Schaetzl et al. 2009), is a measure of long-term soil wetness. It is designed to represent, as an ordinal number, the amount of water that a soil contains and makes available to plants under normal climatic conditions. The higher the DI, the more water the soil can and does, theoretically, supply to plants. Sites with DI values of 99 are essentially open water. A DI of zero indicates impermeable surfaces like bare bedrock or urban areas dominated by pavement and buildings (Schaetzl et al. 2009).

Appendix Table A2. All potential predictive variables and short descriptions included in westside and eastside CART models (source: ClimateNA, 30-year normal period 1990-2020, Wang et al. 2016).

Variable	**Description**
MAT	mean annual temperature (°C)
MWMT	mean warmest month temperature (°C)
MCMT	mean coldest month temperature (°C)
TD	temperature difference between MWMT and MCMT, or continentality (°C)
MAP	mean annual precipitation (mm),
MSP	May to September precipitation (mm),
AHM	annual heat-moisture index (MAT+10)/(MAP/1000))
SHM	summer heat-moisture index ((MWMT)/(MSP/1000))
PAS	precipitation as snow (mm). For individual years, it covers the period between August in the previous year and July in the current year.
EMT	extreme minimum temperature over 30 years
EXT	extreme maximum temperature over 30 years
Eref	Hargreaves reference evaporation (mm)
CMD	Hargreaves climatic moisture deficit (mm)
RH	mean annual relative humidity (%)
CMI	Hogg's climate moisture index (mm)
Seasonal variables and months associated with season (variables below)	Winter (_wt): Dec (prev. yr for an individual year) - Feb for annual, Jan, Feb, Dec for normals
	Spring (_sp): March, April and May
	Summer (_sm): June, July and August
	Autumn (_at): September, October and November
Tmax_wt, sp, sm, at	Winter, spring, summer, autumn mean maximum temperature (°C)
Tmin_ wt, sp, sm, at	winter, spring, summer, autumn mean minimum temperature (°C)
Tave_ wt, sp, sm, at	winter, spring, summer, autumn mean temperature (°C)
PPT_ wt, sp, sm, at	winter, spring, summer, autumn precipitation (mm)
PAS_ wt, sp, sm, at	winter, spring, summer, autumn precipitation as snow (mm)
Eref_ wt, sp, sm, at	winter, spring, summer, autumn Hargreaves reference evaporation (mm)
CMD_ wt, sp, sm, at	winter, spring, summer, autumn Hargreaves climatic moisture deficit (mm)
RH_ wt, sp, sm, at	winter, spring, summer, autumn relative humidity (%)
CMI_ wt, sp, sm, at	winter, spring, summer, autumn Hogg's climate moisture index (mm)

REFERENCES

Crookston, N.L. 2009. Species-Climate Profile for Western redcedar (*Thuja plicata*). Available online (accessed March 2, 2022) at https://charcoal2.cnre.vt.edu/climate/species/speciesDist/Western-redcedar/ or http://forest.moscowfsl.wsu.edu/climate/species/index.php

Hogg, E.H. 1997. Temporal scaling of moisture and the forest-grassland boundary in western Canada. Agricultural and Forest Meteorology 84,115–122.

Hulbert, J. 2022. iNaturalist western redcedar dieback project. Available: https://www.inaturalist.org/projects/western-redcedar-dieback-map

Kabacoff, R.I. 2017. Quick-R by Datacamp: Tree-Based Models. Available online (accessed March 2, 2022) at https://www.statmethods.net/advstats/cart.html

Ma, M. 2014. Classification and Regression Trees (CART) with rpart and rpart.plot. Rpubs by RStudio. Available online (accessed March 2, 2022) at https://rpubs.com/minma/cart_with_rpart

Milborrow, S. 2020. Plotting rpart trees with the rpart.plot package. R Documentation. Available online (accessed March 2, 2022) at http://www.milbo.org/rpart-plot/prp.pdf

Schaetzl, R.J., Krist, F.J. Jr., Stanley, K.E., and C.M. Hupy. 2009. The Natural Soil Drainage Index: An Ordinal Estimate of Long-Term, Soil Wetness. Physical Geography 30:383-409.

The Trust for Public Land. Heat thermal signatures. Available online (accessed March 10, 2022) at https://www.arcgis.com/home/item.html?id=4f6d72903c9741a6a6ee6349f5393572

Van Pelt, R. 2008. Identifying Old Trees and Forests in Eastern Washington. Washington State Department of Natural Resources, Olympia, WA. 166 p.

Wang, T., Hamann, A., Spittlehouse, D.L., and Carroll, C. 2016. Locally Downscaled and Spatially Customizable Climate Data for Historical and Future Periods for North America. PLoS ONE 11(6)